

Lattice distortions in sawtooth chain with Heisenberg and Ising bonds.

Stefano Bellucci¹ and Vadim Ohanyan²

¹*INFN-Laboratori Nazionali di Frascati, Via E. Fermi 40, 00044 Frascati, Italy*

²*Yerevan State University, A.Manooqian, 1, Yerevan, 0025 Armenia*

Yerevan Physics Institute, Alikhanian Br.2, Yerevan, 0036, Armenia

(Dated: June 21, 2024)

An exactly solvable model of the sawtooth chain with Ising and Heisenberg bonds and with coupling to lattice distortion for Heisenberg bonds is considered in the magnetic field. Using the direct transfer-matrix formalism an exact description of the thermodynamic functions is obtained. The ground state phase diagrams for all regions of parameters values containing phases corresponding to the magnetization plateaus at $M = 0, 1/4$ and $1/2$ have been obtained. Exact formulas for bond distortions for various ground states are presented. A novel mechanism of magnetization plateau stabilization corresponding to $M = 1/4$ state is reported.

PACS numbers: 75.10.Pq

I. INTRODUCTION.

The role of lattice distortions in the behavior of magnetic systems continues to be in the focus of intensive theoretical and experimental investigations during last decade. The lift of the ground state degeneracy in frustrated magnets and magnetization plateaus stabilization mechanisms have been investigated intensively in various lattice spin systems with spin–lattice coupling^{1,2,3,4,5,6}. The concept of adiabatic phonons⁷ yielding the effective spin Hamiltonian with additional biquadratic interaction is one of the main approximations using to gain inside into the properties of strongly correlated spin systems, interacting with lattice vibrations. Thus, considering only magnetic properties of the system with spin-lattice interaction, one deals with the Heisenberg model with additional biquadratic terms with coupling constant depending on the parameters of spin-lattice coupling and spring constant of the bond. Also, biquadratic terms can arise in the spin Hamiltonian from the quadrupole-quadrupole interactions. The spin–lattice coupling in quasi-one-dimensional frustrated spin chain, or zigzag ladder, has been shown to generate a series of magnetization plateaus at various rational values of magnetization in addition to one at $M = 1/3$ existing in pure spin system². It was also demonstrated that spin-lattice coupling in zigzag ladder gives rise to a novel type on magnetic excitations carrying fractional spin³. In two-dimensional both classical and quantum spin models with spin–lattice coupling the enhancement of magnetization plateau stabilization as well as appearance of new ordered phases due to biquadratic interaction have been also reported for the $J_1 - J_2 - J_3$ -model⁵ as well as for Shastry–Sutherland lattice⁶ and pyrochlore antiferromagnet¹.

In this paper we consider an exactly solvable one-dimensional spin model with Ising and Heisenberg bonds and spin–lattice interaction between the spins connected with Heisenberg bond. The geometry of the model corresponds to the system known as sawtooth chain. Sawtooth chain, or delta-chain, is one of the prototype examples of

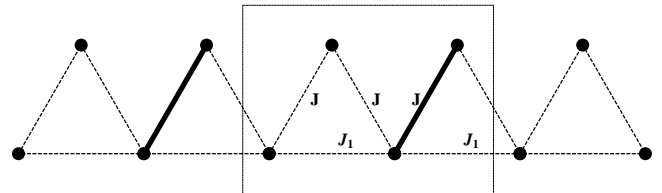


FIG. 1: The sawtooth chain. Heisenberg bonds are marked by thick lines, dashed lines represent Ising bonds. Group of sites pictured into the frame correspond to one block.

highly frustrated lattices. It has a structure of corner-sharing triangles (Fig.(1)). Unlike the other frustrated system, sawtooth chain has peculiar properties such as exactly known dimerized ground state and elementary excitations of quantum soliton type^{8,9,10,11,12}. Significance of the Heisenberg model on sawtooth chain is not limited only to academical interest. Magnetic lattices of few class of materials, such as delafossite $YCuO_{2.5}$ ^{13,14} and olivines with structure ZnL_2S_4 ($L=Er, Tm, Yb$)¹⁵ have been found to be of sawtooth chain type. In addition to that, recently much attention has been paid to the problem of localized magnon states or dispersionless excitation bands, which have been found in various frustrated spin and electron systems, particularly, in the Heisenberg and Hubbard models on sawtooth chain^{16,17,18,19,20,21,22}. Calculating the possible ground state degeneracy corresponding to the localized magnon (or electron in case of Hubbard model) states one can describe low-temperature thermodynamics near saturation field for the corresponding frustrated system^{18,20}. However, exact description of thermodynamic properties for sawtooth chain as well as for many other strongly correlated lattice model is still an open issue. It is worth mentioning two sophisticated methods which allow one to construct thermodynamic functions of integrable model – thermodynamic Bethe ansatz (TBA)²³ and quantum transfer-matrix method (QTM)²⁴, however, applicability of these methods is limited to a very narrow class of integrable systems,

such as XXZ -Heisenberg chain with homogeneous couplings, Hubbard chain, e.t.c. Despite great successes in exact describing of thermodynamic functions for integrable models by TBA and especially by QTM^{25,26}, for many other physically and principally important low-dimensional strongly correlated lattice models only laborious numerical calculations provide more or less reliable results for finite T thermodynamics. Recently, many papers have been devoted to exact solution of the low-dimensional lattice spin models with mixed Ising and Heisenberg bonds^{27,28,29,30,31,32,33,34,35,36,37} or just to pure Ising counterparts of known Heisenberg models with various one-dimensional topologies of bonds^{38,39,40,41,42}. These exact solutions for modified models have much in common with the numerical and experimental results obtained for their Heisenberg counterparts. For instance, an alternating spin-chain with ferromagnetic-ferromagnetic-antiferromagnetic(FFA) interactions has qualitatively the same magnetization curve with magnetization plateau at $M = 1/3$ for Heisenberg⁴³ and Ising spins³⁸. For more complicated F-F-AF-AF chain it has been demonstrated that replacing all ferromagnetic bonds with Ising ones, holding the rest (antiferromagnetic) bonds in original Heisenberg form does not lead to sufficient quantitative changes in the magnetization curve²⁷. The corresponding mixed Ising-Heisenberg F-F-AF-AF chain has been proposed in Ref. [27] as the model of magnetic structure of the compound $\text{Cu}(\text{3-Clpy})_2(\text{N}_3)_2$, where 3-Clpy indicates 3-Chloropyridine. These two examples are the simplest cases of various one-dimensional spin lattice models with clusters of spins interacting with Heisenberg interaction and interacting to each other only through Ising bonds, which have been investigated intensively during

last decade^{27,28,29,30,31,32,33,34,35,36,37}. Partition function and, thus, all thermodynamic functions for such models can be obtained analytically. All these facts allow one to consider these models as an approximation for the underlying quantum spin systems. In Ref. [35] the corresponding approximate model has been considered for the sawtooth chain. In contrast to previous examples, additional features have been observed, namely, magnetization plateau at $M = 1/4$ which is absent in case of purely Heisenberg sawtooth chain. In this paper we perform further investigations of this model complementing it with spin-lattice coupling and giving detailed analysis of all regions of the coupling constants values. The paper is organized as follows: in the Second section the Hamiltonian formulation of the model and its exact solution with classical transfer matrix methods is presented, the zero temperature phase diagrams are obtained in the third section, the fourth section contains an analysis of the average site displacements for different phases, concluding remarks are presented in the last section.

II. HAMILTONIAN AND THERMODYNAMIC FUNCTIONS

We start with considering the sawtooth chain with XXZ Heisenberg bond for the left pair of spins on every second triangle, while all other bonds are taken to be of Ising type. For the sake of brevity, hereafter, we will refer to these bonds as to quantum ones. Beside, each quantum bond is assumed to include elastic energy and displacement depended exchange constant (See Fig. 1). Under these assumptions the Hamiltonian can be decomposed into the sum of block Hamiltonians, commuting to each other:

$$\mathcal{H} = \sum_{i=1}^N \left(\mathcal{H}_i + J\sigma_i\tau_i - H \left(\tau_i + \frac{1}{2}(\sigma_i + \sigma_{i+1}) \right) \right),$$

$$\mathcal{H}_i = J(1 - A\rho_i) (\Delta (S_{i1}^x S_{i2}^x + S_{i1}^y S_{i2}^y) + S_{i1}^z S_{i2}^z) - (H - J_1(\sigma_i + \sigma_{i+1}) - J\tau_i) S_{i1}^z - (H - J\sigma_{i+1}) S_{i2}^z + \frac{K\rho_i^2}{2}, \quad (1)$$

where N is the number of two-triangle blocks in the chain, J_1 and J are coupling constants in the basement and between the side sites and basement respectively, ρ_i is the distortion of quantum bond on i -th block, A is dimensionless spin-lattice coupling and K is the spring constant. Due to commutating block structure of the Hamiltonian

the partition function of the model can be represented in a way, suitable for applying the transfer-matrix formalism. Namely, one can expand the exponential and obtain the product of the terms, with each one corresponding to one block:

$$\mathcal{Z} = \sum_{(\sigma, \tau)} \text{Sp}_{\mathbf{S}} \prod_{i=1}^N \int_{-\infty}^{\infty} \frac{d\rho_i}{2\pi} \exp \left(-\beta \left(\mathcal{H}_i + J\sigma_i\tau_i - H \left(\tau_i + \frac{1}{2}(\sigma_i + \sigma_{i+1}) \right) \right) \right). \quad (2)$$

Here the sum is over all values of Ising variables and $\text{Sp}_{\mathbf{S}}$ stands for the trace over all states of quantum spins, for each quantum bond there is also integral over all possible values of distortion. After implementing integration, one arrives at the effective Hamiltonian with ad-

ditional biquadratic term, which is widely used in the investigations of spin systems with adiabatic coupling to phonons^{1,2,3,4,5,6,7}. Then, trace over quantum states can be taken independently for each block, yielding

$$\mathcal{Z} = \sum_{(\sigma, \tau)} \prod_{i=1}^N \frac{1}{\sqrt{2\pi K\beta}} \text{Sp}[\exp(-\beta \mathcal{H}_i^{eff})] \exp\left(-\beta \left(J\sigma_i\tau_i - H \left(\tau_i + \frac{1}{2}(\sigma_i + \sigma_{i+1}) \right) \right)\right), \quad (3)$$

where effective Hamiltonian reads

$$\begin{aligned} \mathcal{H}_i^{eff} &= J(\mathbf{S}_{i1}\mathbf{S}_{i2})_{\Delta} - b(\mathbf{S}_{i1}\mathbf{S}_{i2})_{\Delta}^2 - (H - J_1(\sigma_i + \sigma_{i+1}) - J\tau_i)S_{i1}^z - (H - J\sigma_{i+1})S_{i2}^z, \\ (\mathbf{S}_{i1}\mathbf{S}_{i2})_{\Delta} &= \Delta(S_{i1}^x S_{i2}^x + S_{i1}^y S_{i2}^y) + S_{i1}^z S_{i2}^z, \end{aligned} \quad (4)$$

And effective constant of biquadratic interaction is given by the relation $b = \frac{J^2 A^2}{2K}$. Then, the partition function of that type can be calculated exactly^{33,34,35} within transfer-matrix formalism. To proceed, one needs to cal-

culate the trace for each block quantum spins, and then to sum over two values of τ_i in each block to give Eq. (3) the standard form corresponding to transfer-matrix technique⁴⁴

$$\begin{aligned} \mathcal{Z} &= \left(\frac{1}{\sqrt{2\pi K\beta}} \right)^N \sum_{(\sigma)} \prod_{i=1}^N T(\sigma_i, \sigma_{i+1}) = \left(\frac{1}{\sqrt{2\pi K\beta}} \right)^N \text{Sp} \mathbf{T}^N, \\ T(\sigma_i, \sigma_{i+1}) &= Z(\sigma_i, \sigma_{i+1}) e^{\beta \frac{H}{2}(\sigma_i, \sigma_{i+1})}, \\ Z(\sigma_i, \sigma_{i+1}) &= \sum_{\tau_i = \pm 1/2} \Omega(\sigma_i, \sigma_{i+1} | \tau_i) e^{-\beta(J\sigma_i - H)\tau_i}, \end{aligned} \quad (5)$$

where

$$\begin{aligned} \Omega(\sigma_i, \sigma_{i+1} | \tau_i) &= \sum_{n=1}^4 e^{-\beta \lambda_n(\sigma_i, \sigma_{i+1} | \tau_i)} = 2e^{\beta \frac{b}{16}} \left(e^{-\beta \frac{J}{4}} \cosh \left(\beta \frac{1}{2} (2H - J(\tau_i + \sigma_{i+1}) - J_1(\sigma_i + \sigma_{i+1})) \right) \right. \\ &\quad \left. + e^{\beta \frac{1}{4}(\Delta^2 b + J)} \cosh \left(\beta \frac{1}{2} \sqrt{(J(\sigma_{i+1} - \tau_i) - J_1(\sigma_i + \sigma_{i+1}))^2 + \Delta^2 \left(J + \frac{1}{2}b \right)^2} \right) \right), \end{aligned} \quad (6)$$

where $\lambda_n(\sigma_i, \sigma_{i+1} | \tau_i)$ are four eigenvalues of \mathcal{H}_i^{eff} :

$$\begin{aligned}\lambda_{1,2}(\sigma_i, \sigma_{i+1} | \tau_i) &= \frac{1}{16} (4J - b) \pm \frac{1}{2} (J(\tau_i + \sigma_{i+1}) + J_1(\sigma_i + \sigma_{i+1})) \mp H, \\ \lambda_{3,4}(\sigma_i, \sigma_{i+1} | \tau_i) &= -\frac{1}{16} (b(1 + 4\Delta^2) + 4J) \mp \frac{1}{2} \sqrt{(J(\sigma_{i+1} - \tau_i) - J_1(\sigma_i + \sigma_{i+1}))^2 + \Delta^2 \left(J + \frac{1}{2}b\right)^2},\end{aligned}\tag{7}$$

The corresponding eigenstates are two polarized vectors with total spin projection $S_{tot}^z = \pm 1$ for $\lambda_{1,2}$ and two

states with $S_{tot}^z = 0$ for $\lambda_{3,4}$:

$$\begin{aligned}|S_{tot}^z = 0, \pm\rangle &= \frac{1}{\sqrt{1 + \gamma_{\pm}^2}} (|\uparrow\downarrow\rangle - \gamma_{\pm} |\downarrow\uparrow\rangle), \\ \gamma_{\pm} &= \frac{J(\sigma_{i+1} - \tau_i) - J_1(\sigma_i + \sigma_{i+1}) \pm \sqrt{(J(\sigma_{i+1} - \tau_i) - J_1(\sigma_i + \sigma_{i+1}))^2 + \Delta^2 \left(J + \frac{1}{2}b\right)^2}}{\Delta \left(J + \frac{1}{2}b\right)}.\end{aligned}\tag{8}$$

Thus, for calculating the partition function of the model, Eq. (5), one should find eigenvalues of the transfer matrix \mathbf{T} ,

$$\mathbf{T} = \begin{pmatrix} e^{\beta \frac{H}{2}} Z_+ & Z_0 \\ \tilde{Z}_0 & e^{-\beta \frac{H}{2}} Z_- \end{pmatrix},\tag{9}$$

where entries are connected with the value of block partition function as follows $Z_+ = Z(1/2, 1/2)$, $Z_0 =$

$Z(1/2, -1/2)$, $\tilde{Z}_0 = Z(-1/2, 1/2)$, $Z_- = Z(-1/2, -1/2)$. Having all that one can easily write the expression for the free energy per block in the thermodynamic limit, when only maximal eigenvalue survives

$$f = -\frac{1}{2\beta} \log \left(\frac{1}{2\pi K\beta} \right) - \frac{1}{\beta} \log \frac{1}{2} \left(e^{\beta \frac{H}{2}} Z_+ + e^{-\beta \frac{H}{2}} Z_- + \sqrt{\left(e^{\beta \frac{H}{2}} Z_+ - e^{-\beta \frac{H}{2}} Z_- \right)^2 + 4Z_0 \tilde{Z}_0} \right).\tag{10}$$

One can see that the first additive term accounts for the vibration contribution to free energy, while effects of interactions between spin degrees of freedom and lattice displacements are incorporated into the b -dependance of the rest part of free energy. After that, all thermodynamic functions can be found exactly by taking corresponding derivatives of free energy. For instance, for magnetization one obtains:

$$M = -\frac{1}{2} \left(\frac{\partial f}{\partial H} \right)_T,\tag{11}$$

III. GROUND STATES AND $T = 0$ PHASE DIAGRAMS

Analyzing possible magnetic ground states of the model under consideration at $T = 0$ one finds large variety of spin configurations with a spacial period equal to the period of the chain. However, there is also another two ground states where translational symmetry is broken up to the period of two blocks. All states can be also classified by the values of magnetization, possible values of which are 0, 1/2 and 1 for states with unbroken translational symmetry, and 0 and 1/4 for the state with doubling of lattice period. Accordingly, the magnetization curves with magnetization plateaus at all

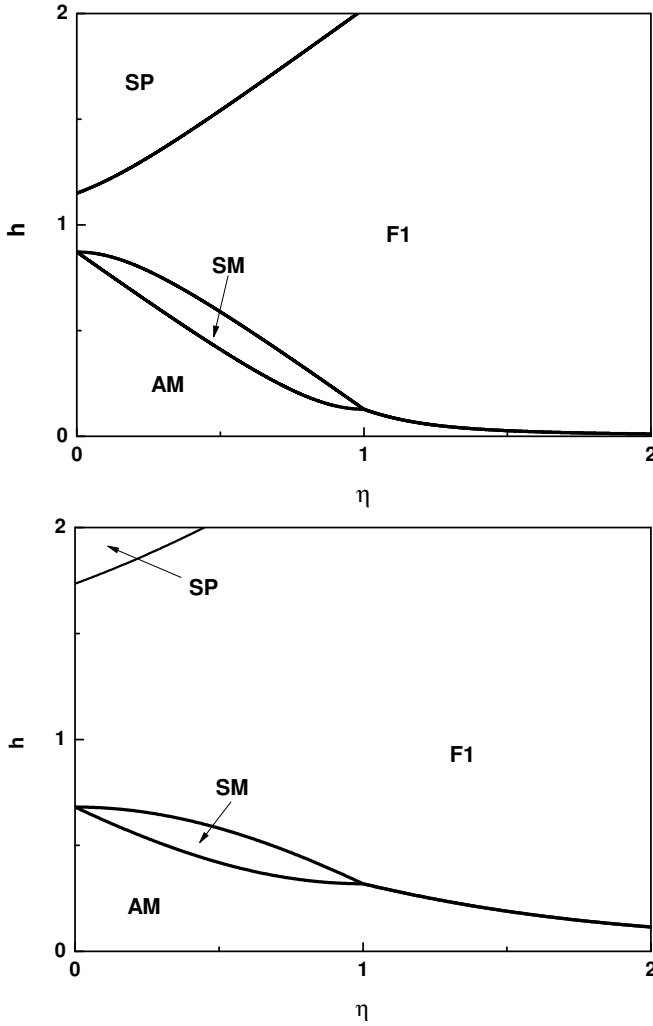


FIG. 2: Ground state $T = 0$ phase diagrams for antiferromagnetic coupling ($J > 0$, $J_1 > 0$) for the sawtooth chain with Ising and Heisenberg bond without biquadratic term (upper panel); and for $b/J = 6$ (lower panel).

aforementioned values of magnetization are expected.

Let us start with antiferromagnetic spin configurations with $M = 0$. There are three antiferromagnetic spin configurations with spacial period equal to lattice period in the system. In the first one all quantum spins are polarized, while both of their adjacent σ and τ spins are pointed in the opposite direction:

$$|AM1\rangle = \prod_{i=1}^N |\uparrow\uparrow\rangle_i \otimes |\sigma_i = \downarrow, \tau_i = \downarrow\rangle, \quad (12)$$

$$\varepsilon_{AM1} = -\frac{1}{16}b - \frac{1}{2}J_1,$$

here ε is the corresponding energy per one block. In another two degenerated by energy antiferromagnetic configurations quantum spins are in the groundstate with $S_{tot}^z = 0$ from Eq. (8) and adjacent Ising spins are pointed oppositely to each other in two different ways:

$$|AM2\rangle = \prod_{i=1}^N |S_{tot}^z = 0, +\rangle_i \otimes |\sigma_i = \uparrow, \tau_i = \downarrow\rangle,$$

$$|AM3\rangle = \prod_{i=1}^N |S_{tot}^z = 0, +\rangle_i \otimes |\sigma_i = \downarrow, \tau_i = \uparrow\rangle,$$

$$\varepsilon_{AM(2,3)} = -\frac{1}{2}J - \frac{1}{16}b(1 + 4\Delta^2) - \frac{1}{2}\sqrt{(J - J_1)^2 + \Delta^2 \left(J + \frac{1}{2}b\right)^2}, \quad (13)$$

where the value of the coefficient γ in the ground state $|S_{tot}^z = 0, +\rangle_i$ is different according to Eq. (8). There is also another antiferromagnetic ground state with broken translational symmetry. In this ground state pairs of

quantum spins are in $|S_{tot}^z = 0, +\rangle$ state while for each block $\sigma_i = \tau_i$ but their joint direction alternates from block to block:

$$\begin{aligned}
|AM4\rangle &= \prod_{i=1}^{N/2} |S_{tot}^z = 0, +\rangle_{2i-1} \otimes |\sigma_{2i-1} = \uparrow, \tau_{2i-1} = \uparrow\rangle \otimes |S_{tot}^z = 0, +\rangle_{2i} \otimes |\sigma_{2i} = \downarrow, \tau_{2i} = \downarrow\rangle, \\
\varepsilon_{AF4} &= -\frac{1}{16}b(1+4\Delta^2) - \frac{1}{2}\sqrt{J^2 + \Delta^2 \left(J + \frac{1}{2}b\right)^2}.
\end{aligned} \tag{14}$$

The system demonstrates also three ferrimagnetic phases with value of magnetization equal to 1/2:

$$\begin{aligned}
|F1\rangle &= \prod_{i=1}^N |S_{tot}^z = 0, +\rangle_i \otimes |\sigma_i = \uparrow, \tau_i = \uparrow\rangle, \\
\varepsilon_{F1} &= -\frac{1}{16}b(1+4\Delta^2) - \frac{1}{2}\sqrt{J_1^2 + \Delta^2 \left(J + \frac{1}{2}b\right)^2} - H, \\
|F2\rangle &= \prod_{i=1}^N |\uparrow\uparrow\rangle_i \otimes |\sigma_i = \downarrow, \tau_i = \uparrow\rangle, \\
\varepsilon_{F2} &= -\frac{1}{16}b - \frac{1}{2}J_1 - H, \\
|F3\rangle &= \prod_{i=1}^N |\uparrow\uparrow\rangle_i \otimes |\sigma_i = \uparrow, \tau_i = \downarrow\rangle, \\
\varepsilon_{F3} &= -\frac{1}{16}b + \frac{1}{2}J_1 - H.
\end{aligned} \tag{15}$$

Finally, let us mention spin polarized, saturated state, where all spins are pointed along the external magnetic field

$$\begin{aligned}
|SP\rangle &= \prod_{i=1}^N |\uparrow\uparrow\rangle_i \otimes |\sigma_i = \uparrow, \tau_i = \uparrow\rangle, \\
\varepsilon_{SP} &= J + \frac{1}{2}J_1 - \frac{1}{16}b - 2H.
\end{aligned} \tag{16}$$

Within some region of the values of system parameters, which is specified below, there is also another state with broken translational symmetry. Namely, this is an inter-

mediate state between $|AM2\rangle$ or $|AM3\rangle$ and $|F1\rangle$ where the σ spins are ordered antiferromagnetically with respect to each other, while all τ spins are pointed along the field. This state can be achieved from $|AM2\rangle$ or $|AM3\rangle$ by flipping every second basement σ spin. We will refer to this state as a spin-modulated state as here the spacial modulation of local spin polarization is occurred along the chain. Namely, local spin polarization of each left pair of spins on each triangle varies in the following way 100010001000..... The corresponding ground state and energy per one block are

$$\begin{aligned}
|SM\rangle &= \prod_{i=1}^{N/2} |S_{tot}^z = 0, +\rangle_{2i-1} \otimes |\sigma_{2i-1} = \uparrow, \tau_{2i-1} = \uparrow\rangle \otimes |S_{tot}^z = 0, +\rangle_{2i} \otimes |\sigma_{2i} = \downarrow, \tau_{2i} = \uparrow\rangle, \\
\varepsilon_{SM} &= -\frac{1}{16}b(1+4\Delta^2) - \frac{1}{4}J - \frac{1}{4}|\Delta \left(J + \frac{1}{2}b\right)| - \frac{1}{4}\sqrt{J^2 + \Delta^2 \left(J + \frac{1}{2}b\right)^2} - \frac{1}{2}H.
\end{aligned} \tag{17}$$

Another one ground state can be appeared in the saw-tooth chain with Ising and Heisenberg bonds without lat-

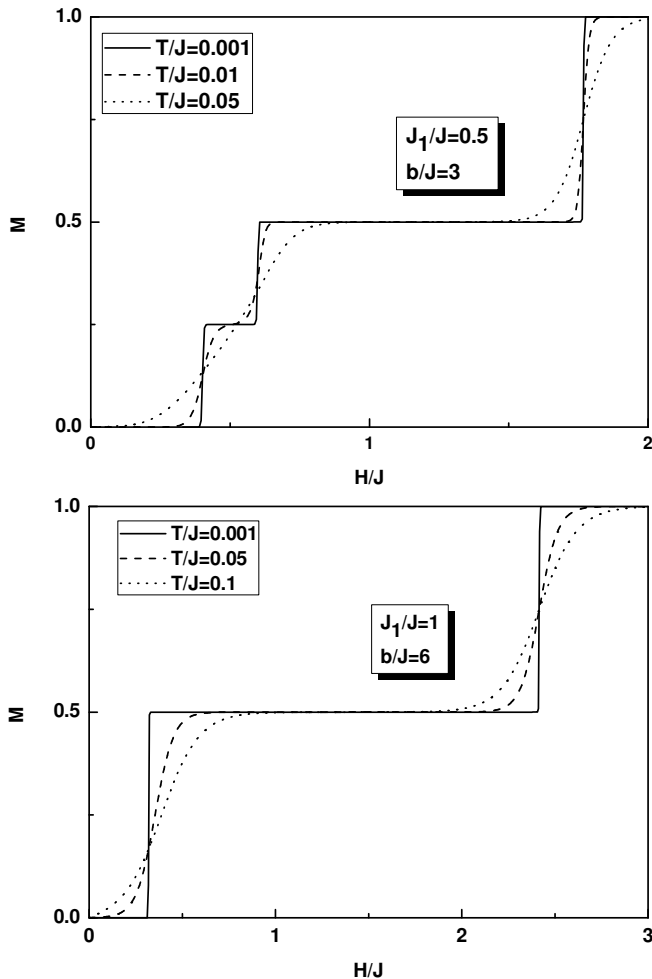


FIG. 3: The plots of magnetization processes for the antiferromagnetic region of interactions, ($J > 0$, $J_1 > 0$), for $\eta = 0.5$ (upper panel) and $\eta = 1$ lower panel for several temperatures. One can see effect of thermal fluctuation on the spin-modulated phase, the plateau at $M = 1/4$ shrink down very rapidly with increasing the temperature, while plateau at $M = 1/2$ is much more stable.

tice distortions³⁵. When $b = 0$ and $J = J_1$ the ground state of the system is a macroscopically twofold degenerated frustrated state

$$|FR\rangle = \prod_{i=1}^N |S_{tot}^z = 0, +\rangle \otimes |\xi_i\rangle, \quad (18)$$

where $|\xi_i\rangle$ stands for either $|\sigma_i = \uparrow, \tau_i = \downarrow\rangle$ or $|\sigma_i = \downarrow, \tau_i = \uparrow\rangle$. Thus, each pair of $\sigma - \tau$ spin in each block are frustrated and can freely pass from one possible state to another.

A. Ground state phase diagram for $J > 0$, $J_1 > 0$

Let us first consider the case of purely antiferromagnetic couplings $J > 0$, $J_1 > 0$. The value of the bi-

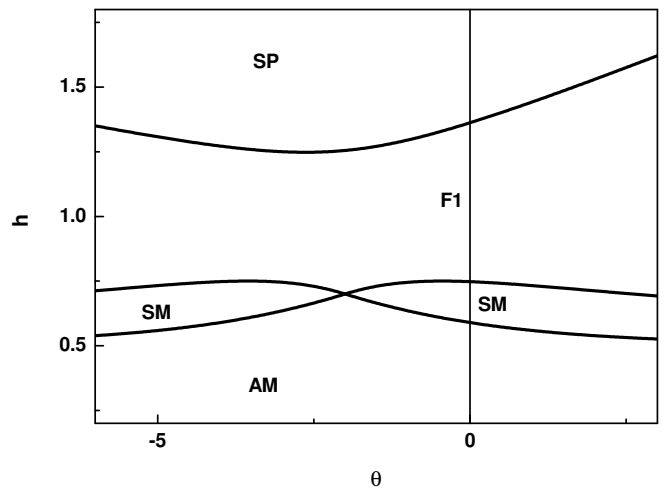


FIG. 4: The ground states phase diagram demonstrating effect of biquadratic terms for $\eta = 0.3$ and $\Delta = 0.3$.

quadratic interaction constant is assumed to be always positive, as $b = \frac{J^2 A^2}{2K}$, $K > 0$. At such values of parameters the system exhibits four different ground states, $|AM2\rangle$ or $|AM3\rangle$ which are degenerated by energies, $|F1\rangle$, $|SM\rangle$, which can appear only at $\eta = J_1/J < 1$ and $|SP\rangle$. When the magnetic field is turned off the ground state of the system at $T = 0$ is always an antiferromagnetic one, corresponding to either $|AM2\rangle$ or $|AM3\rangle$, which are closed analogs of dimerized ground states of conventional quantum sawtooth chain^{8,9,10}. However in exactly solvable model considered here the structure of ground state is more complicated. In contrast to the conventional case where instead of simple dimers, $\frac{1}{\sqrt{2}}(|\uparrow\downarrow\rangle - |\downarrow\uparrow\rangle)$, here one finds $|S_{tot}^z = 0, +\rangle$ states alternating with pairs of oppositely directed Ising spins Eq.(13). Then, with the magnitude of the magnetic field increasing, the sequence of quantum phase transitions takes place, which increase the magnetization of the system in stepwise manner. The corresponding phase diagrams in the (η, h) -plane are presented in Fig. (2), the upper panel demonstrates phase diagram for the sawtooth chain with Ising and Heisenberg bond without lattice distortions, which was previously obtained in Ref. [35], the lower panel demonstrates effects of biquadratic term originated by lattice distortions. Actually, this term enhances the magnetization plateau at $M = 1/2$, which corresponds to the ferrimagnetic phase $|F1\rangle$. The region of phase diagram corresponding to the spin-modulated phase almost is not affected by the value of $\theta = b/J$. This can be explained by the fact, that spin-modulated phase which corresponds to the magnetization plateau at the value $M = 1/4$, appears due to very special structure of the eigenstate of quantum spins with $S_{tot}^z = 0$ which is strongly affected by the values of adjacent Ising spins. Absence of the permutational symmetry in the $|S_{tot}^z = 0, +\rangle$ state and specific dependence of the corresponding eigenvalue on the values of adjacent Ising spins

makes the state with alternating orientation of basement Ising spins stable for certain value of parameters, namely for $\eta < 1$. Thus, this is an example of the novel mechanism of magnetization plateau formation which consists in the doubling of the spacial period of the ground state

due to the difference in effective fields, h_1 and h_2 which act on z -components of two quantum spins in one block, namely $h_1 = H - J\tau_i - J_1(\sigma_i + \sigma_{i+1})$, $h_2 = H - J_1\sigma_{i+1}$. The equations of phase boundaries between four aforementioned phases are:

$$\begin{aligned} \text{between } |AM\rangle \text{ and } |SM\rangle : \quad h &= \frac{1}{2} \left(1 - |D_+(\theta)| - \sqrt{1 + D_+^2(\theta)} \right) + \sqrt{(1 - \eta)^2 + D_+^2(\theta)}, \\ \text{between } |AM\rangle \text{ and } |F1\rangle : \quad h &= \frac{1}{2} \left(1 + \sqrt{(1 - \eta)^2 + D_+^2(\theta)} - \sqrt{\eta^2 + D_+^2(\theta)} \right), \\ \text{between } |SM\rangle \text{ and } |F1\rangle : \quad h &= \frac{1}{2} \left(1 + |D_+(\theta)| + \sqrt{1 + D_+^2(\theta)} \right) - \sqrt{\eta^2 + D_+^2(\theta)}, \\ \text{between } |F1\rangle \text{ and } |SP\rangle : \quad h &= 1 + \frac{1}{2} \left(\eta + \sqrt{\eta^2 + D_+^2(\theta)} \right) + \frac{1}{4} \Delta^2 \theta, \end{aligned} \quad (19)$$

where

$$D_+^2(\theta) = \Delta^2 \left(1 + \frac{1}{2} \theta \right)^2. \quad (20)$$

Two typical plots of magnetization processes corresponding to all antiferromagnetic for different temperatures coupling are presented in Fig. (3), upper panel shows the $\eta < 1$ with three magnetization plateaus at $M = 0, 1/4$ and $1/2$, the lower panel corresponds to the $\eta > 1$ case with only two plateaus at $M = 0$ and $M = 1/2$. As one can see spin-modulated phase is much more sensitive to thermal fluctuations than the rest plateaus, because it is connected with the configuration of Ising spins which is less stable than the entangled state of quantum spins.

Looking at Fig. (2) one can also notice the effect of biquadratic interaction on the length of plateaus. It almost does not affect the plateau at $M = 1/4$ as spin-modulated phase appears due to spin-flip of Ising spins in the basement, however, minor deformations of the region corresponding to the spin-modulated phase can be observed from the phase diagrams. In its turn, biquadratic interaction enhances the plateau at $M = 1/2$ corresponding to $|F1\rangle$ phase as well as the plateau at $M = 0$ corresponding to $|AM(2, 3)\rangle$ phase. The effects of biquadratic term or lattice distortions are summarized in Fig. (4), where the phase diagram in the (θ, h) -plane is presented. One can see almost parallel arrangement of the four phases mentioned above and one peculiar point at $\theta = -2$ where spin-modulated phase disappears. Negative values of b are irrelevant in the model of lattice distortions, as $b = \frac{J^2 A^2}{2K}$ and $K > 0$. However, formally one can consider negative values as well. This effect is obviously

connected with the peculiar properties of Hamiltonian with biquadratic interaction $\mathcal{H} = J_1(\mathbf{S}_1\mathbf{S}_2) + J_2(\mathbf{S}_1\mathbf{S}_2)^2$ at $J_2 = 2J_1$. At this values all four eigenvectors became separable, corresponding just to the standard basis $|\uparrow\uparrow\rangle, |\downarrow\downarrow\rangle, |\uparrow\downarrow\rangle, |\downarrow\uparrow\rangle$, which makes impossible realizations of spin-modulated phase.

B. Ground state phase diagram for $J < 0, J_1 > 0$

Let us consider now another region of the coupling constants values corresponding to ferromagnetic J . In contrast to the previous case here three different ground states are possible at $H = 0$ depending on the value of $\eta = \frac{J_1}{|J|}$. It is interesting to note, that the only one phase with zero magnetization (antiferromagnetic) which appears in this case is $|AF4\rangle$ configuration with broken translational symmetry. Depending of the values of $\theta = \frac{b}{|J|}$ and Δ the ground state phase diagram can have three qualitatively different forms (Fig 5), mainly determined by positions of two special points in η axis. One of them, η_1 , determines the quantum phase transition point between spin polarized and antiferromagnetic $|AF4\rangle$ phases in the absence of magnetic field. Another one, η_2 corresponds to the position of quantum triple point in the (η, h) -plane:

$$\begin{aligned}
\eta_1 &= 2 - \frac{\Delta^2 \theta}{2} - \sqrt{1 + D_-^2(\theta)}, \\
\eta_2 &= \frac{1}{3} \left(\frac{\Delta^2 \theta}{2} - 2 - \sqrt{1 + D_-^2(\theta)} + 2\sqrt{5 + 4\sqrt{1 + D_-^2(\theta)} - \Delta^2 \left(2 + \theta \left(\frac{1}{2}\theta + \sqrt{1 + D_-^2(\theta)} \right) \right) + \frac{\Delta^4 \theta^2}{4}} \right), \\
D_-^2(\theta) &= \Delta^2 \left(1 - \frac{1}{2}\theta \right)^2.
\end{aligned} \tag{21}$$

There is also another special point in the η -axis corresponding to the quantum phase transition point between antiferromagnetic and ferrimagnetic ground states at $H = 0$. This value is parameter independent and is equal to one. When $\eta > 1$ the ground state of the system is $|F1\rangle$. One can see that at positive values of θ always $\eta_1 < \eta_2 < 1$. Thus, when $\eta_1 > 0$ one obtains the ground state phase diagram with spin polarized phase for $\eta < \eta_1$, antiferromagnetic phase $|AF4\rangle$ turning immediately to spin polarized phase under the action of magnetic field for $\eta_1 < \eta < \eta_2$, antiferromagnetic phase $|AF4\rangle$ turning to the ferrimagnetic phase $|F1\rangle$ prior to

spin polarized phase for $\eta_2 < \eta < 1$ and ferrimagnetic phase turning immediately to spin polarized phase for $\eta > 1$. One can see the corresponding phase diagram in the upper panel of Fig. (5). Once η_1 became negative, then one will get another topology of ground state phase diagram presented in middle panel of Fig. (5). And, finally, when η_2 becomes negative only two ground states for $H = 0$ are possible, $|AF4\rangle$ and $|F1\rangle$ and there is no quantum triple point in the phase diagram (lower panel of Fig. (5)). The equations of phase boundaries between three phases occurring in the negative J case are

$$\begin{aligned}
\text{between } |AM4\rangle \text{ and } |F1\rangle: \quad h &= \frac{1}{2} \left(\sqrt{1 + D_-^2(\theta)} - \sqrt{\eta^2 + D_-^2(\theta)} \right), \\
\text{between } |AM4\rangle \text{ and } |SP\rangle: \quad h &= -1 + \frac{1}{2} \left(\eta + \frac{\Delta^2 \theta}{2} + \sqrt{1 + D_-^2(\theta)} \right), \\
\text{between } |F1\rangle \text{ and } |SP\rangle: \quad h &= -1 + \frac{1}{2} \left(\eta + \frac{\Delta^2 \theta}{2} + \sqrt{\eta^2 + D_-^2(\theta)} \right).
\end{aligned} \tag{22}$$

C. Ground state phase diagram for $J > 0$, $J_1 < 0$

At the ferromagnetic value of the coupling constant between the basement spins $J_1 < 0$, the system exhibits rather simple ground states phase diagram with almost parallel arrangement of three phases, $|AF(2,3)\rangle$, $|F1\rangle$ and $|SP\rangle$. The $H = 0$ ground state is always antiferromagnetic which with increase of the external magnetic field magnitude turned to the antiferromagnetic phase with further transition to spin polarized saturated phase. The corresponding phase diagram is presented on Fig. (6). Accordingly, the phase boundaries are given by the same equation as of the purely antiferromagnetic case $J > 0$, $J_1 > 0$ with replacement η by $-\eta$. (See Eq.(19)). Varying parameter of biquadratic interaction b does not lead to a crucial change in the general picture.

IV. AVERAGE DISPLACEMENT

One can easily determine the expression for the equilibrium point of the quantum bond distortion immediately minimizing the block Hamiltonian (1):

$$\hat{\rho}_0 = \frac{JA}{K} (\mathbf{S}_1 \mathbf{S}_2)_\Delta. \tag{24}$$

Thus, in the equilibrium, the distance between sites with quantum spins is determined by their magnetic state. In order to calculate the bond displacement for various ground states one just needs to take quantum-mechanical average of this operator. One can also exploit thermodynamical identities to determine standard deviation of ρ , more precisely

$$\xi = \sqrt{\frac{\sum_{i=1}^N \rho_i^2}{N}} = \sqrt{2 \left(\frac{\partial f}{\partial K} \right)_{T,H}}. \tag{25}$$

On the other hand, one can obtain zero temperature values of distance between the sites with quantum spins just by calculating quantum mechanical averages of the operator $\hat{\rho}_0 = \frac{1}{N} \sum_{i=1}^N \hat{\rho}_{i0}$ for corresponding ground states of the system. For all ground states where pairs of quantum spins are in $|\uparrow\uparrow\rangle$ state, i.e. for $|AM1\rangle$, $|F2\rangle$, $|F3\rangle$ and $|SP\rangle$ one obtains

$$\langle \hat{\rho}_0 \rangle = \frac{JA}{4K}, \quad (26)$$

while for other ground states average distance between quantum spins is given by more complicated expressions depending of the orientation of the other spins of the block. For the ground states with unbroken block-translational symmetry one obtains

$$\rho_0 = \langle \Psi | \hat{\rho}_0 | \Psi \rangle = \quad (27)$$

$$-\frac{JA}{4K} \left(1 + \frac{2\Delta}{\sqrt{1 + \left(\tilde{J}(\tau - \sigma_R) - \tilde{J}_1(\sigma_L + \sigma_R) \right)^2}} \right)$$

where the following notations are adopted

$$\tilde{J} = \frac{J}{\Delta(J + \frac{1}{2}b)}, \quad \tilde{J}_1 = \frac{J_1}{\Delta(J + \frac{1}{2}b)}, \quad (28)$$

and $|\Psi\rangle$ stands for the one of the $|AF(2,3)\rangle$, $|F1\rangle$ ground states, and γ_Ψ is the coefficient from the $|S_{tot}^z = 0, +\rangle$ (Eq. (8)) state calculated for the corresponding values of $\sigma_{L(R)}$ and τ , where $\sigma_{L(R)}$ is the value of the left(right) sigma-spin surrounding quantum spin pairs in the given ground state. For the ground states with block doubling,

$|AM4\rangle$ and $|SP\rangle$ the corresponding expression has the form

$$\langle \Psi | \hat{\rho}_0 | \Psi \rangle = \frac{1}{2} (\rho_1 + \rho_2), \quad (29)$$

where $\rho_{1,2}$ are calculated for the first(second) block in the two-block unit cell of the ground states configuration. Each ρ_i is given by Eq. (27) with corresponding values of $\sigma_{L(R)}$ and τ . In order to compare zero-temperature results with thermodynamically obtained expression form Eq. (25) one needs also to calculate quantum-mechanical averages for the square of operator $\hat{\rho}_0$. Then, one will obtain a quantity thermal average of which coincides with ξ from Eq. (25). Defining $\xi_0 = \sqrt{\langle \Psi | \hat{\rho}_0^2 | \Psi \rangle}$ one will obtain for ground states without translational symmetry breaking

$$\xi_0 = \quad (30)$$

$$\frac{JA}{4K} \sqrt{1 + 4\Delta \left(\frac{1}{\sqrt{1 + \left(\tilde{J}(\tau - \sigma_R) - \tilde{J}_1(\sigma_L + \sigma_R) \right)^2}} + \Delta \right)},$$

and for $|AM4\rangle$ and $|SP\rangle$ phases

$$\sqrt{\langle \Psi | \hat{\rho}_0^2 | \Psi \rangle} = \sqrt{\frac{1}{2} (\xi_1^2 + \xi_2^2)}, \quad (31)$$

where $\xi_{1(2)}$ are calculated according to Eq. (30) for left and right triangles in the block. Below the list of distances between the site with quantum spins for different phases for zero temperature is presented

$$|AM(2,3)\rangle : \quad \rho_0 = -\frac{JA}{4K} \left(1 + \frac{2\Delta}{\sqrt{1 + (\tilde{J} + \tilde{J}_1)^2}} \right), \quad \xi_0 = \frac{JA}{4K} \sqrt{1 + 4\Delta \left(\frac{1}{\sqrt{1 + (\tilde{J} + \tilde{J}_1)^2}} + \Delta \right)}, \quad (32)$$

$$|AM4\rangle : \quad \rho_0 = -\frac{JA}{4K} \left(1 + \frac{2\Delta}{\sqrt{1 + \tilde{J}^2}} \right), \quad \xi_0 = \frac{JA}{4K} \sqrt{1 + 4\Delta \left(\frac{1}{\sqrt{1 + \tilde{J}^2}} + \Delta \right)},$$

$$|F1\rangle : \quad \rho_0 = -\frac{JA}{4K} \left(1 + \frac{2\Delta}{\sqrt{1 + \tilde{J}_1^2}} \right), \quad \xi_0 = \frac{JA}{4K} \sqrt{1 + 4\Delta \left(\frac{1}{\sqrt{1 + \tilde{J}_1^2}} + \Delta \right)},$$

$$|SM\rangle : \quad \rho_1 = -\frac{JA}{4K} \left(1 + \frac{2\Delta}{\sqrt{1 + \tilde{J}^2}} \right), \quad \rho_2 = -\frac{JA}{4K} (1 + 2\Delta), \quad \rho_0 = -\frac{JA}{4K} \left(1 + \Delta \left(1 + \frac{1}{\sqrt{1 + \tilde{J}^2}} \right) \right),$$

$$\xi_1 = \frac{JA}{4K} \sqrt{1 + 4\Delta \left(\frac{1}{\sqrt{1 + \tilde{J}^2}} + \Delta \right)}, \quad \xi_2 = \frac{JA}{4K} \sqrt{1 + 4\Delta(1 + \Delta)}, \quad \xi_0 = \frac{JA}{4K} \sqrt{1 + 2\Delta \left(\frac{1}{\sqrt{1 + \tilde{J}^2}} + 2\Delta \right)}.$$

Magnetic field dependence of the standard deviation of the distance between lattice sites with quantum spins

given by Eq. (25) is presented in Fig. (7). One can see

low temperature step-like changes of ξ according to the connection between site distance and magnetic state of spin situated at them (Eq. (24)).

V. CONCLUDING REMARKS

In this paper we presented a complete analysis of the magnetic properties of the sawtooth chain with Ising and Heisenberg bond and spin–lattice coupling for spins interacting with Heisenberg interaction. After integration over site displacements one deals with the additional biquadratic spin interaction. Due to special arrangement of Ising and Heisenberg bonds exact calculation of partition function of the system has been performed. The system exhibits large variety of ordered phases, among which are those with the doubling of the unit cell. Magnetic behavior of the system is also rather rich. Depending of the values of parameters, coupling constant in the basement J_1 , coupling constant for the interaction between spins on the top and basement spins J and effective coupling constant of additional biquadratic interaction b , various magnetization curves are possible with magnetization plateaus at $M = 0, 1/4$ and $1/2$. Let us mention, that exact diagonalization calculations for ordinary antiferromagnetic sawtooth chain at $J = 2J_1$ reported in Ref. [21], revealed only one plateau at $M = 1/2$, which corresponds to the so-called magnon crystal, an eigenstate with whole filling of all possible localized magnon states. In our case, the microscopic physical origin of this plateau state is completely different due to special structure of the interactions. However, at corresponding values of coupling constants (the left half of the phase diagram presented in Fig. (2) in upper panel) the system with mixed Ising and Heisenberg bonds considered here exhibits magnetization curve with all three magnetization plateaus mentioned above. Special attention should be paid to the magnetization plateau at $M = 1/4$. The origin of the corresponding eigenstate $|SM\rangle$ is in the nonequivalence of the left and right σ spin for each pair of quantum spins, provided later are in the $|S_{tot}^z = 0, +\rangle$ state in which \mathbf{S}_1 and \mathbf{S} in their turn are nonequivalent. Thus, at a certain value of external magnetic field magnitude, the eigenstate with doubling of the unit cell becomes stable, in which σ spins in the left and right blocks of the doubled unit cell are in different states. To our knowledge, this is the

novel mechanism of magnetization plateau stabilization inherent in the systems with mixed Ising and Heisenberg bonds. The same arguments are valid for the antiferromagnetic state with doubling unit cell $|AF4\rangle$. Generally speaking, the same mechanism can be presented in the purely quantum models with inhomogeneous interaction. For sawtooth chain, one can consider the model where coupling constants in the basement, on the left leg and on the right leg of the triangles, are all different, or consider the model with alternating interaction in the basement. Probably, for some values of coupling constant the magnetic behavior of such a sawtooth chain will have much in common with that shown here for model with Ising and Heisenberg bonds, particularly, magnetization plateau at $M = 1/4$. This issue requires further investigation in order to clarify the deep connections between magnetic and thermodynamic properties of quantum spin models and their Ising-Heisenberg counterparts. There is surprisingly good correspondence between magnetization curves of quantum F-F-AF-AF alternating chain and the same chain with ferromagnetic bonds changed with the Ising ones obtained in Ref. [27]. This, as well as other results^{27,28,29,30,31,32,33,34,35,36,37,38,39,40,41,42}, allows one to consider the change of interaction bonds with Ising ones for providing exact solvability, as an approximate methods in theory of strongly correlated spin lattice models. An especially good agreement can be achieved when only ferromagnetic bonds are changed with Ising ones, because the ground state of two ferromagnetically interacting spins is the same for Ising and for Heisenberg interaction. While, for antiferromagnetically interacting spins quantum ground state is spin singlet which is an entangled state which has no direct analogies in case of Ising interaction. Thus, changing antiferromagnetic bond with Ising one leads to crucial loose of important physical properties, while for ferromagnetic coupling the physical difference is not so pronounced.

Acknowledgments

V.O. expresses his gratitude to LNF-INFN for hospitality during the work on the paper and acknowledges partial support form the grants CRDF-UCEP - 06/07 and ANSEF-1518-PS.

¹ K. Penc, N. Shannon, and H. Shiba, Phys. Rev. Lett. **93**, 197203 (2004).
² T. Vekua, D. C. Cabra, A. Dobry, C. Gazza, and D. Poilblanc, Phys. Rev. Lett. **96**, 117205 (2006).
³ C. Gazza, A. Dobry, D. Cabra, and T. Vekua, Phys. Rev. B **75** 165104 (2007).
⁴ D. C. Cabra, M. Moliner, and F. Stauffer, Phys. Rev. B **74**, 014428 (2006).
⁵ S. Bissola, V. Lante, A. Parola, and F. Becca, Phys. Rev.

B **75**, 184444 (2007).
⁶ S. Miyahara, F. Becca, and F. Mila, Phys. Rev. B **68**, 024401 (2003).
⁷ C. Kittel, Phys. Rev. **120**, 335 (1960).
⁸ K. Kubo, Phys. Rev. B **48**, 10 552 (1993).
⁹ T. Nakamura and K. Kubo, Phys. Rev. B **53**, 6393 (1996).
¹⁰ D. Sen, B. S. Shastry, R. E. Walstedt, and R. Cava, Phys. Rev. B **53**, 6401 (1996).
¹¹ T. Nakamura and S. Takada, Phys. Lett. A **225**, 315

- (1997).
- ¹² S. A. Blundell and M. D. Núñez–Regueiro, *Eur. Phys. J. B* **31**, 453 (2003).
 - ¹³ R. J. Cava, H. W. Zandbergen, A. P. Ramirez, H. Takagi, C. T. Chen, J. J. Krajewski, W. F. Peck, Jr., J. V. Waszczak, G. Meigs, R. S. Roth, and L. F. Schneemeyer, *J. Solid State Chem.*, **104**, 437 (1993).
 - ¹⁴ O. Le Bacq, A. Pasturel, C. Lacroix, M. D. Núñez–Regueiro, *Phys. Rev. B* **71**, 014432 (2005).
 - ¹⁵ G. C. Lau, B. G. Ueland, R. S. Freitas, M. L. Dahlberg, P. Schiffer, and R. J. Cava, *Phys. Rev. B* **73**, 012413 (2006).
 - ¹⁶ A. Honecker, O. Derzhko, J. Richter, *Ground–state degeneracy and low–temperature thermodynamics of correlated electrons on highly frustrated lattices*, [arXiv: 0903.3296].
 - ¹⁷ J. Richter, J. Schulenburg, A. Honecker, J. Schnak, H.-J. Schmidt, *J. Phys.: Condens. Mater* **16**, S779 (2008).
 - ¹⁸ O. Derzhko, A. Honecker, J. Richter, *Phys. Rev. B* **76**, 220402(R) (2008).
 - ¹⁹ O. Derzhko, J. Richter, A. Honecker, *Low. Temp. Phys.* **33**, 745 (2007).
 - ²⁰ J. Richter, O. Derzhko, A. Honecker, *Int. J. Mod. Phys. B* **22**, 4418 (2008).
 - ²¹ J. Richter, J. Schulenburg, A. Honecker, J. Schnack, and H.-J. Schmidt, *J. Phys.: Condens. Matter* **16**, S779 (2004).
 - ²² J. Schulenburg, A. Honecker, J. Schnack, J. Richter, and H.-J. Schmidt, *Phys. Rev. Lett.* **88**, 167207 (2002).
 - ²³ M. Takahashi, *Thermodynamics of One-dimensional Solvable Models*, (Cambridge: Cambridge University Press) 1999.
 - ²⁴ A. Klümper, *Lect. Notes Phys.* 645, 349-379 (2004).
 - ²⁵ A. Klümper, *Eur. J. Phys. B* **5**, 677 (1998).
 - ²⁶ C. Trippé, A. Honecker, A. Klümper, and V. Ohanyan, *Exact Calculation of the Magnetocaloric Effect in the spin-1/2 XXZ-chain*, [arXiv:0908.XXXX](2009)
 - ²⁷ J. Strečka, M. Jaščur, M. Hagiwara and K. Minami, Y. Narumi, and K. Kindo *Phys. Rev. B* **72**, 024459 (2005).
 - ²⁸ J. Strečka and M. Jaščur, *J. Phys. : Condens. Matter* **15**, 4519 (2003).
 - ²⁹ L. Čanová, J. Strečka and M. Jaščur, *J. Phys. : Condens. Matter* **18**, 4967 (2006).
 - ³⁰ J. Strečka, L. Čanová, T. Lučivjanský, and M. Jaščur, *J. Phys.: Conf. Ser.* **145**, 012058 (2009).
 - ³¹ L. Čanová, J. Strečka, T. Lučivjanský, *Exact solution of the mixed spin-1/2 and spin-S Ising-Heisenberg diamond chain*[arXiv: 0903.4566](2009).
 - ³² J. S. Valverde, O. Rojas, and S. M. de Souza, *J. Phys.: Condens. Matter* **20**, 345208 (2008).
 - ³³ D. Antonosyan, S. Bellucci, V. Ohanyan, *Phys. Rev. B* **79**, 014432 (2009).
 - ³⁴ V. Ohanyan, *Phase diagrams of the Ising-Heisenberg chain with S=1/2 triangular XXZ clusters*, [arXiv: 0812.0127](2008).
 - ³⁵ V. Ohanyan, *Antiferromagnetic sawtooth chain with Heisenberg and Ising bonds*, [arXiv: 0905.4776](2009).
 - ³⁶ M. S. S. Pereira, F. A. B. F. de Moura, and M. L. Lyra, *Phys. Rev. B* **77**, 024402 (2008).
 - ³⁷ M. S. S. Pereira, F. A. B. F. de Moura, and M. L. Lyra, *Phys. Rev. B* **79**, 054427 (2009).
 - ³⁸ V. Ohanyan and N. Ananikian, *Phys. Lett. A* **307**, 76 (2003).
 - ³⁹ F. Litaiff, J. de Sousa, and N. Branco, *sol. state commun.* **147**, 494 (2008).
 - ⁴⁰ V. Ohanyan and N. Ananikian, in *MATHEMATICAL PHYSICS Proceedings of the XI Regional Conference Tehran, Iran 2004* ed. by S Rahvar, N Sadooghi and F Shojai, p.49-51 (World Scientific)(2005).
 - ⁴¹ E. Aydiner and C. Akyüz, *Chin. Phys. Lett.* **22**, 2382 (2005).
 - ⁴² E. Aydiner, C. Akyüz, M. Gönülol, and H. Polat, *phys. stat. sol(b)* **243**, 2901 (2006).
 - ⁴³ K. Hida, *J. Phys. Soc. Jpn.* **63**, 2359 (1994).
 - ⁴⁴ R. Baxter, *Exactly Solved Models in Statistical Mechanics*, (Academic Press, New York, 1982).

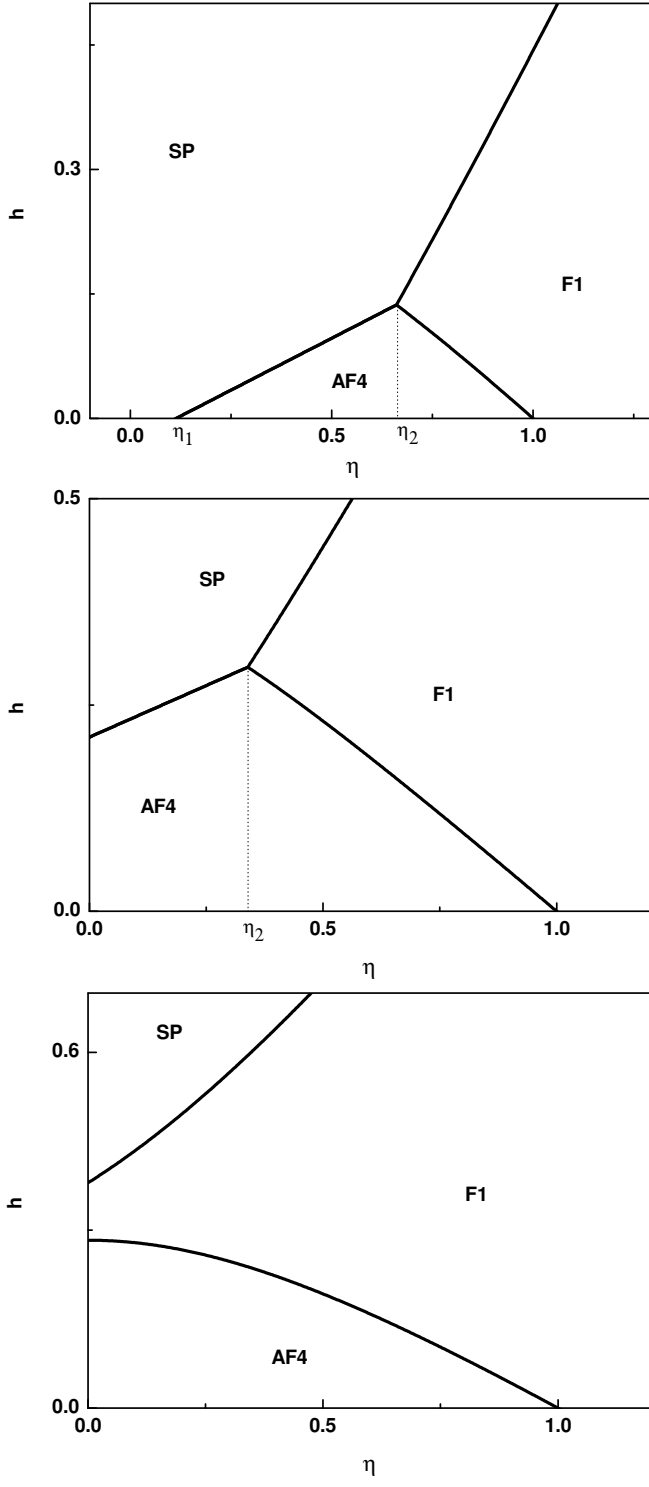


FIG. 5: The ground states phase diagram for $J = -1$, $\Delta = 1.2$ and $b = 1$ (upper panel), $b = 2.5$ (middle panel) and $b = 3$ (lower panel). Here $h = H/|J|$.

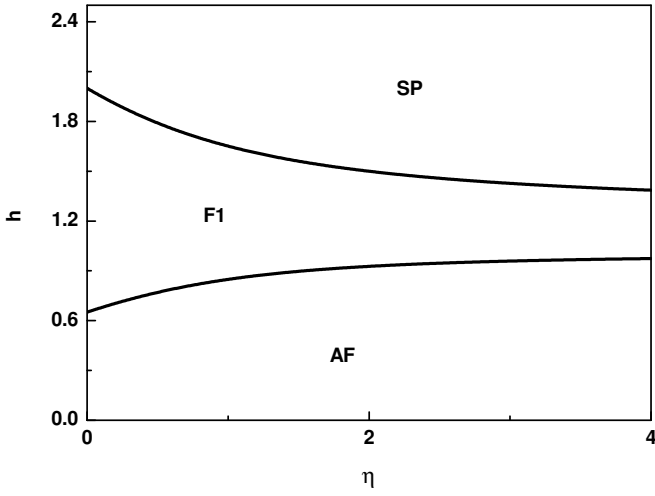


FIG. 6: The ground states phase diagram for $J_1 = -1$, $J = 1$, $b = 1$ and $\Delta = 1$. Here $\eta = |J_1|/J$, $h = H/J$.

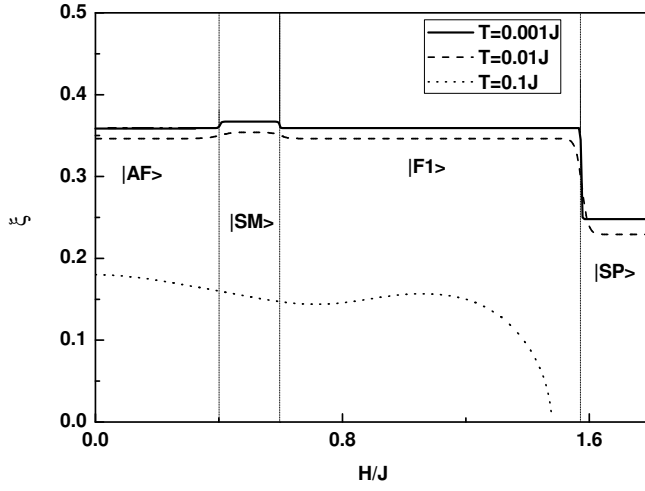


FIG. 7: Standard deviation of the distance between sites with quantum spins vs. external magnetic field magnitude for three different temperatures and $J = 1$, $J_1 = 0.5$, $b = 0.5$ and $\Delta = 0.3$. Regions of different ground states corresponding to $T = 0$ phase diagram are separated from each other by horizontal thin lines.